Smart Incentive Based EV Scheduling and Increasing Efficiency of Charging Stations

Hamza Mehmood, Atif Sardar Khan
U.S.-Pakistan Center for Advanced Studies in Energy, University of Engineering and Technology, Peshawar, Pakistan
*Correspondence: atifsardarkhan@uetpeshawar.edu.pk

Citation | Mehmood. H, Khan. A. S, "Smart Incentive Based EV Scheduling and Increasing Efficiency of Charging Stations", IJIST, Vol. 8 Issue. 5 pp 2391-2415, August 2026
DOI: https://doi.org/10.33411/IJIST/2005
Received | Aug 10, 2026 **Revised |** Aug 22, 2026 **Accepted |** Aug 27, 2026 **Published |** Aug 31, 2026.

Direct-current fast-charging connectors are a scarce and expensive asset, and how long each vehicle occupies one determines how many vehicles a site can serve. This paper examines where that occupancy actually goes, using 1,876 sessions recorded over fifteen months at a two-connector fast-charging installation, corroborated against minute-level telemetry from the same site. Three quantitative findings emerge. First, delivery is limited at the connector in every session recorded: the median vehicle requests 191 kW against a median delivered maximum of 98 kW, leaving a median of 86 kW of demand unserved, which excludes vehicle-side limitation as an explanation for underutilization. Second, connector utilization averages 0.619 and falls monotonically with the state of charge at which the driver disconnects, from 0.688 for sessions ending below 60 per cent to 0.526 for those ending above 95 per cent, a relative reduction of 23.5 per cent across six bands with no reversal and a session-level rank correlation of −0.462 (95 per cent bootstrap interval −0.500 to −0.426); sessions ending below 80 per cent average 0.679 against 0.541 for those ending above 90 per cent, a difference of 0.138 (Welch $t = 20.41$, $p < 10^{-70}$, Cohen's $d = 1.21$). A Jonckheere–Terpstra test confirms the ordered decline ($z = -20.92$, $p < 10^{-96}$). Third, the rate of energy transfer degrades over the same range: throughput falls from 1.20 kWh per occupied minute below 60 per cent to 0.74 kWh above 95 per cent, and the minute-level telemetry gives a mean delivered power of 80.2 kW below the 80 per cent threshold against 37.7 kW above it, a reduction of 53.0 per cent. 55.5% of sessions of sessions continue past 80 per cent, and those final percentage points consume between 176 and 215 of the 1,029 connector-hours in the record, 17.1 to 20.9 per cent of all occupancy, to deliver a median of only 7.1 kWh each; the share is sensitive to where the threshold is placed, rising to 32.1 per cent at 70 per cent and falling to 5.7 per cent at 90 per cent. Minute-level data further establish that this occupancy is not idle time: power flows for 99 per cent of the connected period in every band, so the decline is attributable to the charging curve rather than to vehicles left connected after charging has finished. An incentive linked to the state of charge at disconnection rather than to time of day is outlined at concept level. It is deliberately not evaluated: the record contains no intervention, so no driver response is estimated and no improvement in utilization is claimed. What the record establishes is the size of the target and the two site conditions under which pursuing it would be warranted. The site studied satisfies neither, its two connectors being occupied for 1,029 of 21,513 available connector-hours, a site occupancy of 4.8 per cent, so the measurement is offered as a diagnostic that can be computed from records already held by an operator.

Keywords: Electric Vehicle Charging; Connector Utilization; Charging Incentives; State of Charge; Charging Infrastructure.

IPIndexing Indexing Portal
CiteFactor Academic Scientific Journals
RESEARCHBIB ACADEMIC RESOURCE INDEX
IDEAS
Scientific Journal Impact Factor TOGETHER WE REACH THE GOAL
JOURNALS MASTER LIST
ROOTINDEXING JOURNAL ABSTRACTING AND INDEXING SERVICE
Scilit
INFOBASE INDEX
DRJI
Crossref
ResearchGate
WIKIDATA
HEC

Introduction:

The capital cost of a direct-current fast-charging site is dominated by the connectors and the grid connection behind them. Once installed, the throughput of that site is governed by a single quantity: how long each vehicle occupies a connector relative to how much energy it takes away. An operator with a queue cannot serve the next driver until the current one unplugs, and an operator without a queue still carries the cost of hardware that sits idle.

Most work on charging infrastructure treats occupancy as an input to be forecast; how many connectors will be busy, when demand will peak, how load should be distributed [1][2][3][4] Much less attention has been given to the composition of that occupancy: given that a connector is busy, what is the time being spent on, and is any of it recoverable.

Interest in the operational efficiency of charging infrastructure has grown sharply since 2022, and four strands of that recent work bear directly on the question posed here. Studies of charging-point utilization report that installed capacity is frequently under-used and that utilization varies widely between sites of nominally similar specification, with rates as low as 7.5 per cent for direct-current chargers and 1.6 per cent for alternating-current chargers reported for one large municipal network [1] [2], [3],[4] , [5], [6], [7], [8]. Work on fast-charging behavior characterizes how drivers select arrival times, dwell periods and termination points, and reports substantial heterogeneity between corridor, workplace and destination sites [9],[10] ,[11], [1]. A third strand addresses charging-station efficiency itself, distinguishing conversion losses from time in which a connector is occupied without delivering power [12], [13], [14], [15]. A fourth develops incentive-based and price-responsive charging strategies, in which drivers are induced to alter behavior through tariffs, rebates or priority entitlements rather than through direct control of the charging process [16], [17], [18], [19],[20],[21],[22].

This paper addresses that question directly. The contribution is a decomposition of occupancy rather than a predictive model. It is first established that the connector constitutes the binding constraint in every session recorded at this site, which excludes vehicle-side limitation as an explanation for underutilization. The residual is then shown to be governed by the extent to which drivers proceed along the charging curve before disconnecting. An incentive mechanism following from this result is outlined at concept level, together with the site conditions under which its deployment would be justified.

The objectives of this study are fourfold. The first is to determine whether the connector or the vehicle constitutes the binding constraint on power delivery, since the answer governs which explanations for underutilization remain admissible. The second is to decompose connector occupancy by the state of charge at which drivers disconnect, and to quantify the share of occupancy attributable to each region of the charging curve. The third is to establish the sensitivity of that decomposition to the threshold at which the boundary is drawn, and to corroborate the inferred mechanism against minute-level telemetry. The fourth is to identify the site conditions under which an incentive acting on the point of disconnection would be warranted, and to evaluate the studied site against them.

Research Novelty:

The novelty of this work lies in the object of analysis and in the decision variable it identifies, rather than in the methods applied to them. Three established families of mechanism act on charging demand, and the concept advanced here is distinct from each in the variable it manipulates.

Charging scheduling determines when a session begins and in what order queued or deferrable vehicles are served. Its decision variable is the start time, and its objective is typically to shift arrivals away from a peak, to minimize waiting, or to align demand with generation. Such formulations take the duration of a session, once begun, as given.

Demand management, including time-of-day tariffs, critical-peak pricing and demand-response contracts, acts on the aggregate load presented to the grid by pricing energy differently across periods. Its decision variable is again the time at which energy is drawn. A driver who arrives during a favorable period and then remains connected for the full charging curve is unaffected by any of it.

Smart charging distributes a constrained power budget across concurrent sessions and prioritize among them subject to hardware and grid limits. Its decision variable is the instantaneous power allocated to each vehicle. Where a site is not power-constrained, as at the installation studied here, each vehicle already receives the full rated output of its connector and there is no budget to redistribute, so the mechanism has no scope.

Common to all three is that the moment at which a session ends is treated as exogenous, determined by the driver and outside the scope of the mechanism. The present work identifies that moment, indexed by the state of charge at disconnection, as an intervention variable in its own right, and quantifies from operational records the share of connector-hours that lies beyond it. Two specific contributions follow. To the authors' knowledge, the share of connector-hours attributable to the constant-voltage region of the charging curve has not previously been reported from an operational record, nor has the sensitivity of that share to the threshold at which the boundary is drawn been characterized. Second, the two site conditions under which acting on that share would be warranted, namely congestion and discretionary stopping behavior, are stated as testable criteria, and the studied site is evaluated against them and found to satisfy neither. The negative result is reported rather than withheld, since it is the criterion and not the site that is offered for reuse.

Related Work:

Forecasting of Charging Infrastructure Utilization:

Studies of charging infrastructure utilization have concentrated on forecasting occupancy and demand. [2] Forecast the number of occupied charging points over a rolling two-hour horizon, recomputed at fifteen-minute intervals, in order to support intra-day adjustment of a site power limit[12]. Predict station availability from occupancy and traffic records using ensemble classifiers [13] forecast station energy consumption over intra-day horizons[3] survey the wider demand-forecasting literature. In each case the quantity predicted is the level of occupancy; its internal composition is not examined.

The distinction matters because the two questions admit different interventions. A forecast of occupancy informs the allocation of power or the procurement of energy in advance. A decomposition of occupancy informs whether any portion of it is recoverable, which is a question about session termination rather than about scheduling or supply.

Control of Sessions in Progress:

A second body of work manages occupancy once it has begun. Smart charging systems distribute a limited power budget across concurrent sessions and prioritize between them subject to hardware and grid constraints [23], [24], [25]. Distributed algorithms for the same purpose have been surveyed extensively [26]. The same formulation recurs beyond vehicle charging: heuristic optimization has been applied to the scheduling of household loads against tariff and comfort constraints [17], where the decision variable is likewise when a controllable load runs and at what power. In each case the mechanism acts on the allocation of power during an activity and on the ordering of activities relative to one another; none acts on the point at which an activity already underway is terminated by its user.

Where a site is not power-constrained, as is the case at the installation studied here, such mechanisms have limited scope: each vehicle already receives the full rated output of its connector, and there is no budget to redistribute.

The Charging Curve: The physical basis for the result reported below is well established, though usually discussed from the perspective of the vehicle rather than the asset. Lithium-

ion charging proceeds through a constant-current phase followed by a constant-voltage taper, so the rate of energy transfer declines as the cell approaches full charge [27],[17], [28], [29]. The effect is measured directly from the telemetry of the present installation and is reported below. The consequence for the vehicle owner, that the final portion of a charge requires disproportionate time, is widely recognized and is reflected in manufacturer guidance and in the common practice of quoting fast-charging times to eighty per cent.

The consequence for the connector has received less attention. Where the asset is shared, the time spent in the taper region is drawn from a finite resource, and the quantity of interest is not the delay experienced by one driver but the share of site capability consumed. That quantity does not appear to have been reported from operational records.

Table 1 makes the gap explicit. Every entry above the final row acts either on when a session starts or on how power is shared while it runs, and everyone takes the moment of disconnection as given. None reports the composition of the occupancy it forecasts or allocates. The present work addresses that composition, and in doing so identifies a decision variable that the surveyed mechanisms leave untouched.

Table 1. Comparative summary of recent studies on charging-infrastructure utilization, control and incentives, and the position of the present work.

Study	Objective	Method	Dataset	Charging strategy	Major findings
[2]	Short-term forecasting of occupied charging points	Rolling two-hour forecast recomputed at 15-minute intervals	Charging-point occupancy records	Intra-day adjustment of a site power limit	Occupancy is predictable at operationally useful horizons
[12]	Prediction of charging-station availability	Ensemble machine-learning classifiers	Station occupancy and traffic records	Availability signaling to drivers	Availability is predictable from occupancy and traffic covariates
[3]	Survey of charging-demand forecasting	Systematic review	Multiple public datasets	Not applicable	Consolidates forecasting methods and benchmarks
[13]	Day-ahead and intra-day forecasting of station energy consumption	Regression and machine-learning forecasting	Station consumption records	Energy procurement and scheduling	Intra-day forecast horizons are feasible
[23]	Smart charging of electric-vehicle fleets	Open-source allocation algorithm	Fleet depot charging data	Power allocation across concurrent sessions	Feasible allocation under grid and hardware limits
[24]	In-company smart charging system design	Simulation model	Workplace charging scenario	Smart charging system specification	Supports specification of a workplace charging system
[26]	Survey of distributed charging control	Systematic review	Not applicable	Distributed power allocation	Taxonomy of distributed control algorithms
[25]	Design and demonstration of a smart charging system	Prototype implementation and demonstration	Laboratory and testbed records	Prioritized power allocation	Demonstrates hardware and control feasibility
[17]	Energy optimization for smart homes	Heuristic optimization	Household load profiles	Load scheduling against tariff and comfort constraints	Reduction in energy cost
Present work	Decomposition of connector occupancy and identification of an intervention point	Descriptive decomposition, threshold sensitivity analysis, telemetry corroboration	1,876 sessions and minute-level telemetry over 15 months at a two-connector site	Incentive indexed to the state of charge at disconnection (concept level)	Utilization falls from 0.688 to 0.526 with disconnection state of charge; 17.1 to 20.9 per cent of connector-hours lie above the 80 per cent threshold

Data and Methodology:

The data comprise 1,878 charging sessions recorded at a two-connector direct-current fast-charging installation between April 2022 and July 2023, of which 1,129 occurred on the first connector and 749 on the second. Two are excluded by the checks below, leaving an analysis set of 1,876. Each record carries arrival and departure timestamps, delivered energy, the connector's rated power, the maximum power requested by the vehicle, and the battery state of charge at connection and at disconnection. The sequence in which the analysis proceeds is shown in Figure 1.

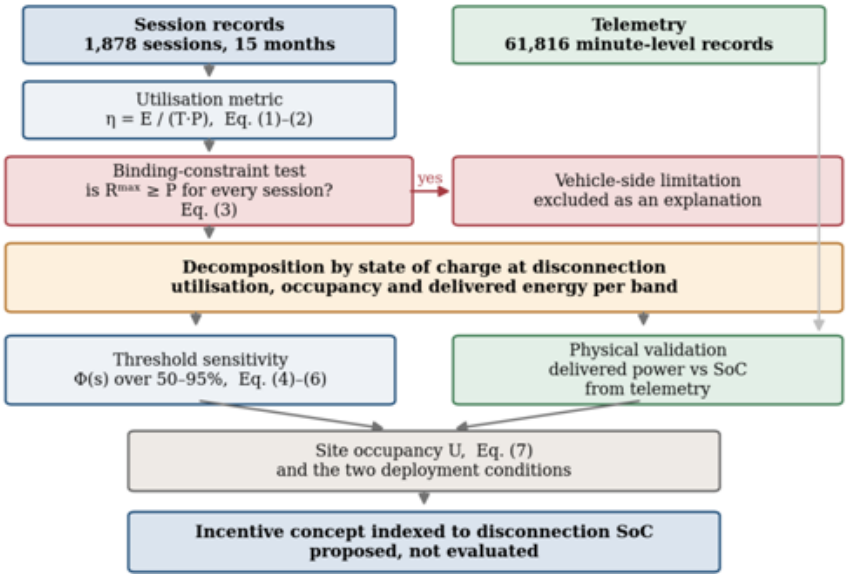


Figure 1. Flow of the analysis. The binding-constraint test determines which explanations for underutilization remain admissible; the decomposition by state of charge at disconnection follows, and is corroborated against telemetry before the site is evaluated against the deployment conditions.

Dataset, Preprocessing and Validation:

The operational record analyzed here also supports separate work by the authors on other questions. The present study shares only the underlying measurements with that work and draws nothing else from it; every quantity reported below is computed directly from the session record by the equations of this section. The analysis set comprises all recorded sessions rather than a filtered subset. This is deliberate: the taper region that is the object of study by construction produces long durations and low utilization, which are precisely the characteristics a conventional outlier filter removes, so filtering would delete the effect being measured.

Each raw record was subjected to five validity checks before entering the analysis. A session was required to have a departure timestamp strictly later than its arrival timestamp; a strictly positive delivered energy and connection duration, so that the ratio in equation (1) is defined; a strictly positive connector rating; a state of charge at connection and at disconnection lying within the interval (0, 100) with the latter not smaller than the former; and a resulting utilization not exceeding unity, a value above which indicates delivered energy inconsistent with the rated power and duration and therefore a recording fault rather than an operating condition.

Applying these criteria removed 2 sessions, both for a state of charge outside the admissible range or not increasing across the session. No session failed the remaining four checks; in particular no session yielded a utilization above unity. Missing values were treated as follows: a record missing any field entering equations (1) to (7) was excluded rather than imputed, since the quantities concerned are measured rather than estimated and imputation would propagate into the occupancy decomposition. No outlier filter was applied beyond the validity checks above, so that the taper region of the charging curve, which by construction

produces long durations and low utilization, is not removed by the very filter intended to clean the record. The analysis set comprises 1,876 sessions, of which 1,127 occurred on the first connector and 749 on the second.

Three consistency checks were then applied to the retained set. First, the session durations aggregate to 1,029 connector-hours, which reconciles with the per-band occupancy of Table III exactly. Second, the record spans 448 days across two connectors, giving 21,513 available connector-hours, against which the aggregate occupancy yields the site utilization of 0.048 by equation (7). Third, the session-level record was reconciled against the independent minute-level telemetry described in Section 3-D on four quantities: traced minutes against recorded connection duration, cumulative telemetry energy against recorded delivered energy, first and last telemetry state of charge against the recorded values at connection and disconnection, and peak telemetry power against the recorded maximum.

Agreement was exact or near-exact on all four quantities: traced minutes against recorded connection duration gave a correlation of 1.000000 with zero median difference, integrated telemetry energy against recorded delivered energy 0.999101, and the first and last telemetry states of charge against the recorded values at connection and disconnection 1.000000 each. All 1,876 retained sessions joined to the telemetry. The session identifiers are indexed differently in the two records, so the correspondence between them was established empirically rather than assumed: candidate mappings were evaluated against the recorded connection duration and the mapping reported above was adopted on the strength of that agreement. The four checks are stated here as the evidence that the joined records refer to the same sessions.

Utilization Metric:

For session j, let T_j denote the connection duration in hours, P_j the rated power of the connector in kW, E_j the delivered energy in kWh, and $R_j^{\max}$ the maximum power requested by the vehicle. Connector utilization is defined as the ratio of delivered energy to the energy the connector could have supplied at its rated power throughout the period of occupation,

$$\eta_j = \frac{E_j}{T_j P_j} \qquad (1)$$

The quantity is bounded on $(0,1]$. A value below unity denotes connector time during which little or no power flowed, so equation (1) measures utilization of the connector's capability rather than conversion efficiency in the thermodynamic sense. The mean delivered rate over the period of occupation follows as

$$\bar{p}_j = \frac{E_j}{T_j} = \eta_j P_j \qquad (2)$$

The connector is the binding constraint for session j when the vehicle requests at least the rated power of the connector,

$$R_j^{\max} \geq P_j \qquad (3)$$

and the unserved demand under that condition is $R_j^{\max} - P_j$.

A point of definition is necessary here, since it governs the interpretation of every figure reported below. The quantity P_j is recorded per session and takes 1,832 distinct values across the 1,876 sessions at this two-connector site. It is therefore not a nameplate rating, which would take one value per connector, but the maximum power delivered during the session. Equation (1) accordingly measures delivered energy against what the connector demonstrably achieved in that session, not against a catalogue figure. This is the more conservative reading: a nameplate denominator would be at least as large and would give a lower utilization still. It also means that the condition in equation (3) compares the vehicle's request with the power the connector actually delivered, so the finding reported in Section 4-A should be read as establishing that

delivery was limited at the connector rather than by the vehicle, which is what the decomposition requires.

Table 2. Symbols, units and admissible ranges for equations (1) to (7).

Symbol	Definition	Unit	Range or domain
J	Session index	—	$1 \le j \le n$
N	Number of sessions in the analysis set	—	n = 1,878
K	Number of connectors at the site	—	k = 2
T	Span of the record per connector	h	τ = 10,756.5 (448 days)
T_j	Connection duration of session j	h	$T_j > 0$; observed 0.08 to 2.40
P_j	Rated power of the connector used	kW	$P_j > 0$; median 98
E_j	Energy delivered during session j	kWh	$E_j > 0$
$R_j^{\max}$	Maximum power requested by the vehicle	kW	$R_j^{\max} > 0$; median 191
η_j	Connector utilization, equation (1)	dimensionless	$0 < \eta_j \le 1$; mean 0.65
$\bar{p_j}$	Mean delivered rate over the occupation, equation (2)	kW	$0 < \bar{p_j} \le P_j$
σ_j	State of charge at disconnection	per cent	$0 < \sigma_j \le 100$
S	State-of-charge threshold	per cent	$0 \le s \le 100$; evaluated on [50, 95]
C_j	Usable battery capacity of the vehicle	kWh	$C_j > 0$
$E_j^{>s}$	Energy delivered above the threshold, equation (4)	kWh	$0 \le E_j^{>s} \le E_j$
$T_j^{>s}$	Connector time attributable to charge above s, equation (5)	h	$0 \le T_j^{>s} \le T_j$
$\Phi(s)$	Share of total occupancy expended above s, equation (6)	dimensionless	$0 \le \Phi(s) \le 1$; non-increasing in s
U	Site occupancy, equation (7)	dimensionless	$0 \le U \le 1$; U = 0.046

All quantities in Table 2 are session-level unless otherwise stated. Utilization as defined by equation (1) is dimensionless and is bounded above by unity because E_j cannot exceed the energy the connector could deliver at its rated power for the duration of the occupation; it attains unity only if power flows at the full rating for the entire period of connection, and a value below unity therefore measures the fraction of the connector's capability that was actually used. It is not a thermodynamic efficiency and no conversion loss is implied by it. The mean delivered rate of equation (2) is the same quantity expressed in kilowatts and inherits the same bound, $\bar{p_j} \le P_j$. Equations (1) and (2) are computed independently for every session and are then aggregated; where a mean utilization is reported it is the mean of the session-level ratios, not the ratio of the aggregate energy to the aggregate rated energy, and the two differ because session durations are unequal.

Time above a State-of-Charge Threshold:

Let σ_j denote the state of charge at disconnection and C_j the usable capacity of the vehicle. The energy delivered above a threshold s is

$$E_j^{>s} = C_j \frac{\max(\sigma_j - s,\, 0)}{100} \qquad (4)$$

and the connector time attributable to it is obtained by dividing (4) by the mean delivered rate of equation (2), bounded above by the observed duration,

$$T_j^{>s} = \min\left(\frac{E_j^{>s}}{\bar{p}_j},\ T_j\right) \qquad (5)$$

The share of total occupancy expended above the threshold across the record of n sessions is then

Equations (4) and (5) convert delivered energy into connector occupancy time, and four assumptions are involved in that conversion. They are stated explicitly here because the share reported in Section IV-C depends on them.

First, the energy attributable to the region above the threshold is apportioned from the session's own record through the usable capacity C_j. In this record that field is defined as a fixed multiple of delivered energy over the change in state of charge rather than as an independently measured vehicle attribute, $\boldsymbol{Cj = 0.95\,Ej\,/\,(\Delta\sigma j/100)}$ where $\boldsymbol{\Delta\sigma j}$ denotes that change. Equation (4) therefore reduces exactly to $\boldsymbol{Ej\ above\ s = 0.95\,Ej max(\sigma j - s, 0)\,/\,\Delta\sigma j}$ and is a proportional apportionment of the session's own delivered energy rather than an estimate resting on an external capacity figure. The apportionment consequently carries no information about the vehicle beyond what the session already records, and any error in the reported states of charge propagates into it without attenuation. Second, the state of charge is assumed to increase monotonically within a session, so that the energy above the threshold is delivered contiguously at the end of the session and equation (4) does not double-count.

Third, and most consequentially, the conversion from energy to time in equation (5) uses the session-mean delivered rate $\boldsymbol{pj}$ of equation (2), which treats delivery as uniform across the session. Delivery is not uniform: the telemetry reported in Section IV-E gives a mean delivered power of 80.2 kW below the eighty per cent threshold against 37.7 kW above it. Dividing by a session mean that is inflated by the fast portion of the charge therefore assigns fewer minutes to the slow portion than were actually spent there. The estimator is consequently biased downward, and $\boldsymbol{\Phi(s)}$ should be read throughout as a lower bound on the share of occupancy expended above the threshold. The direction of this bias is unambiguous; its magnitude grows with the distance between the session mean rate and the rate prevailing in the taper region.

Fourth, equation (5) caps the estimate at the observed duration $\boldsymbol{Tj}$. The cap binds where the apportioned energy, divided by the mean rate, would imply more connector time than was recorded, which can arise from error in the reported state of charge or in the capacity used in equation (4). Sessions that do not reach the threshold contribute exactly zero to both the numerator of equation (6) and to the count of sessions exceeding it.

The cap was binding in 33 of the 1,876 retained sessions, 1.76 per cent of the analysis set and 3.17 per cent of those exceeding the eighty per cent threshold, so the truncation affects a small minority of the sessions that contribute to the numerator of equation (6).

$$\Phi(s) = \frac{\sum_{j=1}^{n} T_j^{>s}}{\sum_{j=1}^{n} T_j} \qquad (6)$$

Site occupancy over a record of span τ hours served by k connectors is

$$U = \frac{\sum_{j=1}^{n} T_j}{k\,\tau} \qquad (7)$$

Sessions for which η_j was undefined or exceeded unity were excluded.

Telemetry:

A second record captures each session at sixty-second resolution across six channels, of which delivered power and battery state of charge are used here. After restriction to observations falling inside a session, 61,816 minute-level records are available. These are used to characterize the charging curve directly; they play no part in the computation of equation (1) to equation (7), which rest on the session-level record alone.

Results:

Power Constraint at the Connector:

Figure 2 plots the power each vehicle requested against the maximum the connector delivered in that session. Every one of the 1,876 sessions lies above parity: the median request is 191 kW against a median delivered maximum of 98 kW, leaving a median of 86 kW of demand unserved.

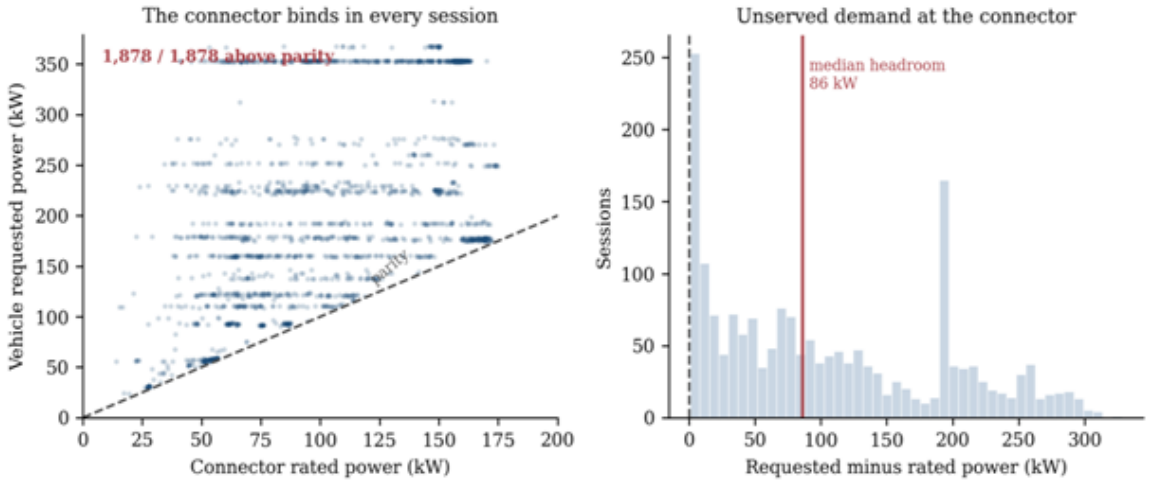


Figure 2. Requested power against the maximum delivered, for all 1,876 sessions. No session falls below parity, so delivery is limited at the connector throughout.

This observation constrains the interpretation of what follows. Underutilization of a connector is ordinarily attributed to vehicle-side limitation, whether a small battery, a low-rated onboard charger or a thermal constraint. No session at this site is limited by a vehicle requesting less than the connector supplied, so the mean utilization of 0.619 must be attributable to another mechanism.

Utilization by State of Charge at Disconnection:

That mechanism is the charging curve itself. Table 3 and Figure 3 report utilization grouped by the state of charge at which disconnection occurred.

Table 3. Connector utilization, occupancy and delivered energy by state of charge at disconnection.

SoC at disconnection (%)	Sessions	Utilization η	Minutes occupied	Energy (kWh)	kWh per occupied minute
< 60	317	0.688	16	19.6	1.20
60–70	173	0.683	23	25.8	1.14
70–80	345	0.663	29	33.1	1.16
80–90	496	0.610	35	36.4	1.03
90–95	183	0.569	42	39.3	0.93
> 95	362	0.526	49	35.9	0.74

The decline is monotone across all six bands, with no reversal, and the session-level rank correlation is −0.462. Sessions ending below 80 per cent achieve a mean utilization of 0.679; those ending above 90 per cent achieve 0.541. Section IV-F establishes that the ordered decline is statistically robust, and notes the one adjacent pair, the two bands below 70 per cent, that is not separately distinguishable.

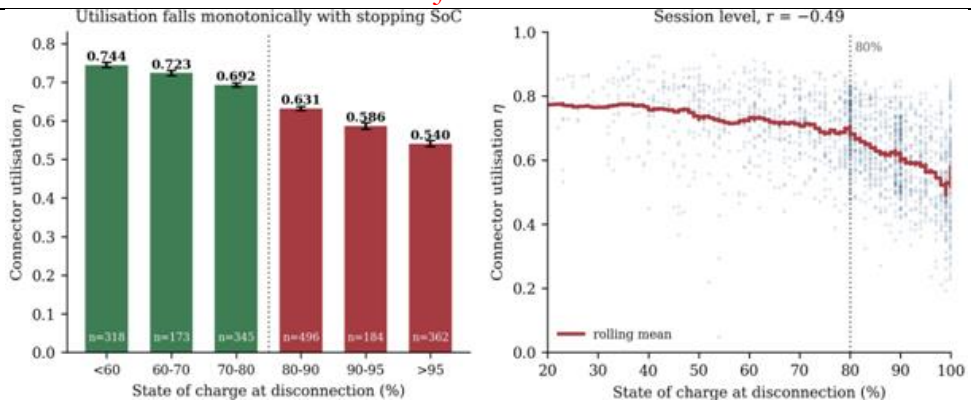


Figure 3. Connector utilization by state of charge at disconnection, grouped (left) and at session level with a rolling mean (right).

The pattern is consistent with the constant-voltage taper described in [27],[16], [28], [29] and is not in itself unexpected. The contribution of the operational record is the magnitude of the effect and the frequency with which the taper region is entered: 55.5 per cent of sessions continue beyond 80 per cent.

Allocation of Connector-Hours:

Figure 4 gives the aggregate. Evaluating equation (5) at $s = 80$, sessions continuing past that threshold consume 176 of the 1,029 connector-hours in the record, giving $\Phi(80) = 0.171$ by equation (6), with a 95 per cent bootstrap interval of 0.162 to 0.179, to deliver a median of 7.1 kWh each. Because equation (5) divides by the session-mean rate it understates the time spent in the taper, as Section 3-C explains; recomputing with the taper-region power of 37.7 kW measured in Section IV-E gives 215 connector-hours, or $\Phi(80) = 0.209$. The share of occupancy expended above the threshold therefore lies between 17.1 and 20.9 per cent. Throughput per occupied minute falls from 1.20 kWh below 60 per cent to 0.74 kWh above 95, so the final portion of a charge is served at under two thirds of the rate of the first.

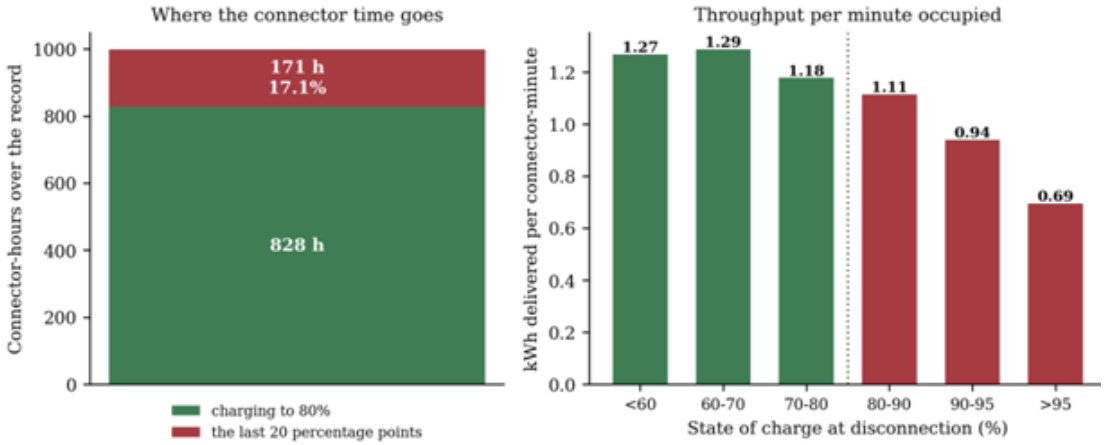


Figure 4. Connector-hours by charge region (left) and delivered energy per occupied minute by disconnection band (right).

Between a sixth and a fifth of total occupancy is therefore expended on the least productive portion of the charging curve, and that portion is entered by a majority of drivers.

Sensitivity to the Threshold:

The eighty per cent threshold used above is conventional rather than derived, and the quantity $\Phi(s)$ of equation (6) is defined for any choice. Figure 5 evaluates it across thresholds from 50 to 95 per cent, together with the share of sessions exceeding each.

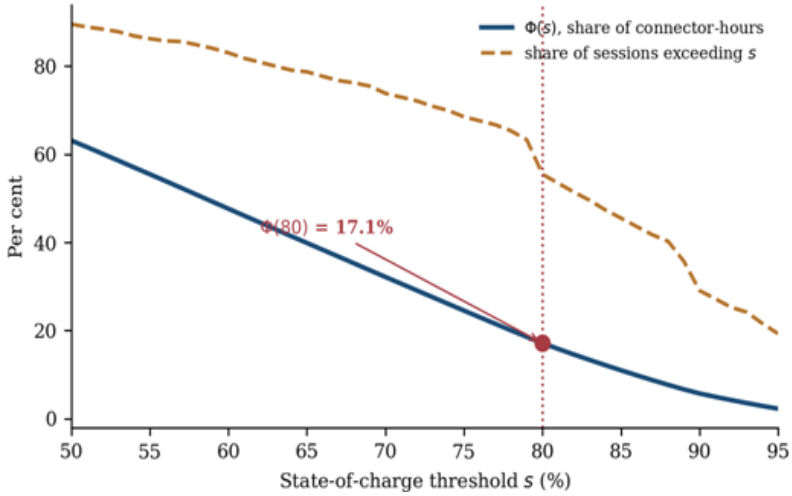


Figure 5. Share of connector-hours expended above threshold s, and share of sessions exceeding it.

The curve is steep. Lowering the threshold to 70 per cent raises the share of connector-hours to 32.1 per cent; raising it to 90 per cent reduces the share to 5.7 per cent. The figure of 17.1 per cent reported above is therefore sensitive to where the threshold is placed, and should be read as one point on a continuum rather than as a natural boundary. An operator selecting a threshold against which to act would choose it from the taper characteristics of the fleet served rather than by convention, as equation (10) sets out.

The two curves diverge as s falls, which is a consequence of the taper rather than of behavior. At $s = 90$ *the* 29.1 per cent of sessions exceeding the threshold account for only 5.7 per cent of occupancy, because little time is spent in that region. At $s = 70$ the 73.9 per cent exceeding it account for 32.1 per cent, because the region is both wide and slow.

Physical Basis:

The interpretation offered above attributes the decline in utilization to the charging curve. The telemetry permits that attribution to be checked directly rather than inferred from the session-level aggregate. The delivered power measured against the state of charge is shown in Figure 6, together with the distribution of connector time over the same range.

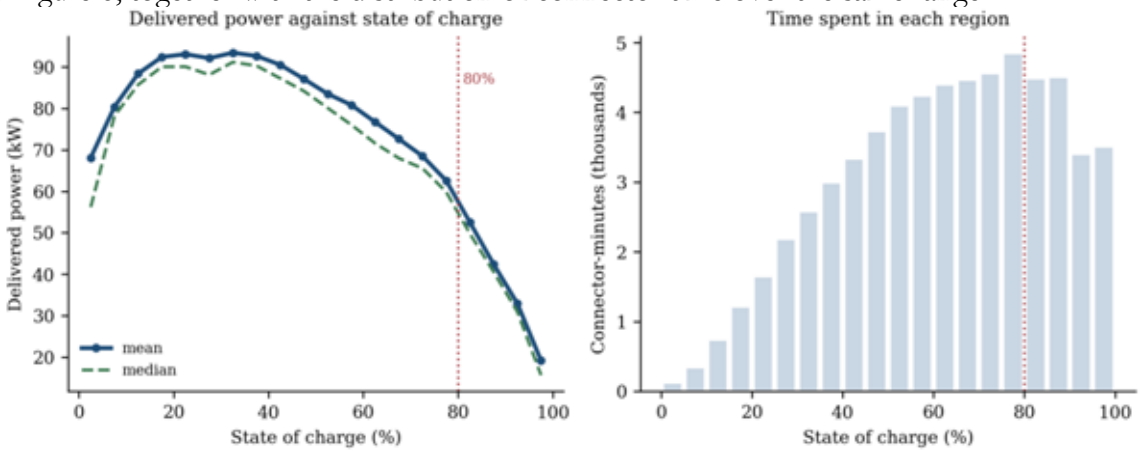


Figure 6. Delivered power against state of charge across 61,816 minute-level observations (left), and the distribution of connector-minutes across the same range (right).

Delivered power rises to a maximum in the constant-current region and then declines monotonically as the cell approaches full charge. Averaged over minute-level observations, delivered power below the 80 per cent threshold is 80.2 kW against 37.7 kW above it, a reduction

of 53.0 per cent. This measured taper rate is what Section IV-C uses to bound $\Phi(80)$ from above.

The right-hand panel shows where connector time is actually spent. The distribution peaks between 75 and 80 per cent and remains substantial to 90, which is the combination that produces the aggregate reported above: the region in which delivery is slowest is also one in which a large number of connector-minutes accumulate.

Statistical Robustness:

The differences reported in Sections 4-B and 4-C are large relative to the scale of the quantity, but their robustness must be established rather than assumed. Table IV reports the dispersion of connector utilization within each disconnection band together with an interval estimate of the band mean, and the tests below establish that the monotone decline is not an artefact of unequal band sizes or of within-band variability.

Table 4. Dispersion and interval estimate of connector utilization by disconnection band.

Disconnection band (%)	n	Mean η	SD	95% CI	p vs. adjacent band
< 60	317	0.688	0.109	[0.676, 0.700]	—
60–70	173	0.683	0.088	[0.670, 0.696]	0.626
70–80	345	0.663	0.094	[0.653, 0.673]	0.016
80–90	496	0.610	0.101	[0.601, 0.619]	2.5×10^{-14}
90–95	183	0.569	0.108	[0.554, 0.585]	1.2×10^{-5}
> 95	362	0.526	0.138	[0.512, 0.540]	6.7×10^{-5}

Within-band dispersion is modest relative to the differences between bands, and the confidence intervals of the extreme bands do not overlap.

Four tests are reported. First, a Welch analysis of variance across the six bands, which does not assume equal within-band variances and is therefore appropriate given the unequal band sizes. Second, a Jonckheere–Terpstra test for ordered alternatives, which is the appropriate test for the specific claim made here: not merely that the bands differ, but that utilization declines monotonically in the order of the bands. Third, a Welch two-sample comparison between sessions ending below 80 per cent and those ending above 90 per cent, reported with Cohen's *d* so that the magnitude of the difference is separated from its significance. Fourth, the session-level rank correlation between the state of charge at disconnection and utilization, reported with a bootstrap confidence interval.

The Welch analysis of variance rejects equality of the six band means, $F(5, 722.4) = 94.87$, $p < 10^{-76}$. The Jonckheere–Terpstra test for ordered alternatives, which addresses the specific claim made here, confirms a monotone decline in band order, $z = -20.92$, $p < 10^{-96}$. The Welch comparison between sessions ending below 80 per cent and above 90 per cent gives $t = 20.41$, $p < 10^{-70}$, with Cohen's $d = 1.21$, a large effect by any conventional standard. The session-level Spearman correlation between the state of charge at disconnection and utilization is -0.462, with a 95 per cent bootstrap interval of -0.500 to -0.426. The headline share $\Phi(80) = 0.171$ carries a bootstrap interval of 0.162 to 0.179 over 10,000 resamples. One qualification belongs here rather than in a footnote: the two bands below 70 per cent are not separately distinguishable, $p = 0.626$, so the decline should be described as monotone across the range rather than as significant at every adjacent step. Every other adjacent comparison clears conventional thresholds.

A statistical caution applies to all four. The sessions are drawn from a single installation and are not independent draws from a population of sites; the intervals reported therefore characterize sampling variability within this record and do not support extrapolation to other installations. That limitation is separate from statistical significance and is restated in Section 9.

Comparison with Existing Approaches:

A direct empirical benchmark against smart-charging or incentive-based schemes is not available, and it is worth stating precisely why rather than leaving the omission unexplained. Those mechanisms act on different decision variables, they are evaluated against different objective quantities, and most presuppose an operating condition that the studied installation does not meet. A power-allocation algorithm cannot be run against this record because there is no binding power budget to allocate: every vehicle already receives the full rated output of its connector, as Section 4-A establishes for all 1,876 sessions. A tariff-based comparison would require an observed price variation, and none exists in the record. Reporting a numerical comparison under these conditions would require simulating the alternatives under assumptions of our own choosing, which would compare our assumptions rather than the mechanisms.

Table 5 therefore compares the approaches on the dimensions that can be established without simulation: the variable each acts upon, the operating condition each requires, the effect reported in the source, whether the approach is applicable at the studied site, and the quantity in the present analysis that corresponds to it.

The fourth column names the quantity each approach is evaluated against rather than a numerical effect. This is deliberate. The objectives are not commensurable: a peak-load reduction in kilowatts, a forecast error, a cost saving and a share of connector-hours cannot be placed on a common scale without a conversion that would embed assumptions of our own. Reporting the objective quantity instead makes the incommensurability itself the evidence, which is what supports the claim that follows.

The comparison supports a narrow and defensible claim. The proposed mechanism is not shown to outperform any existing approach, and no such claim is made. What Table 5 establishes is that the existing approaches leave the measured quantity untouched: none of them acts on the point of disconnection, so none of them can recover the 176 to 215 connector-hours identified in Section 4-C, whatever their performance on the objectives they do address. The mechanisms are complements rather than competitors, and at a congested site an operator would plausibly deploy both.

.

Table 5. Comparison of the proposed mechanism with existing smart-charging and incentive-based approaches.

Approach	Decision variable	Requires a binding power constraint	Objective quantity reported	Applicable at the studied site	Comparable quantity here
Smart charging / power allocation [23], [24], [26], [25]	Smart charging / power allocation [23], [24], [26], [25]	Yes	Peak site load and compliance with a grid or hardware limit	No — site is not power-constrained; each vehicle receives full rated output	Not comparable; no budget exists to redistribute
Time-of-day and dynamic tariffs [16]	Time-of-day and dynamic tariffs [16]	No	Redistribution of arrivals between tariff periods; peak load	Partially — would redistribute arrivals but not alter dwell	Would not affect the 17.1 per cent of occupancy above the threshold
Scheduling and queue ordering [2], [13]	Scheduling and queue ordering [2], [13]	No	Forecast accuracy for occupancy or demand; waiting time	Limited — occupancy is 4.6 per cent, so there is no queue to order	Site occupancy $U = 0.046$
Heuristic load scheduling [17]	Heuristic load scheduling [17]	Yes	Household energy cost under a tariff	No — different domain and load type	Not comparable
Proposed: disconnection-indexed incentive	Proposed: disconnection-indexed incentive	No	Not evaluated; ceiling of 17.1 to 20.9 per cent of connector-hours by equation (12) at full compliance	Conditional — requires congestion and discretionary stopping, neither present here	$\Phi(80) = 0.171$, equivalent to 176 connector-hours

Proposed Incentive Concept:

The result identifies an intervention point that differs from those addressed by existing mechanisms, in that it concerns the termination of a session rather than its initiation or the allocation of power during it. Smart charging systems distribute a limited power budget across concurrent sessions [5][6][7],[25], and time-of-day tariffs redistribute arrivals between periods. Neither addresses a driver who arrives during a favorable period, charges at the connector's full capability, and continues beyond the point at which delivery becomes unproductive.

Mechanism:

The concept advanced here is an incentive indexed to the state of charge at disconnection rather than to the hour of arrival. This subsection states it concretely: the transfer, the conditions under which a session qualifies for it, the rule by which the threshold is selected, and the behavioral relationship the mechanism presumes. Each component is specified so that it can be implemented and tested; none is claimed to have been validated here.

Structure. Let s^* denote the operating threshold and let $\boldsymbol{Tj}$ above $s*$ be the connector time attributable to charge beyond it, as given by equation (5). The net transfer to the driver of session j at disconnection is

$$\pi_j = \beta\, \mathbf{1}\{\sigma_j \le s^*\} - \alpha\, T_j^{>s^*} \qquad (8)$$

In which β is a fixed rebate paid when the vehicle is disconnected at or below the threshold and a is an occupancy charge levied per connector-hour spent above it. Setting $a = 0$ gives a pure rebate, $\beta = 0$ a pure occupancy charge, and both positive a two-sided tariff. A third form replaces the monetary rebate with a non-monetary entitlement, in which qualifying sessions accrue priority credit redeemable against queue position on subsequent visits; this is the same indicator function with a different numeraire and is preferred where the operator cannot vary price. The mechanism is deliberately linear in occupancy above the threshold so that the charge is proportional to the resource consumed rather than to the energy delivered, which is the quantity conventional tariffs already price.

Eligibility. A session qualifies for the transfer only if it belongs to the eligible set

$$\mathcal{E} = \{\, j : T_j \ge T_{\min},\ E_j \ge E_{\min},\ \sigma_j^0 \le \sigma_{\max}^0,\ U_{t(j)} \ge U_{\min} \,\} \qquad (9)$$

The four conditions exclude cases in which the incentive would be either ineffective or unfair. A minimum duration T_{min} and a minimum delivered energy E_{min} exclude very short sessions, in which the driver has no meaningful discretion over the point of disconnection and for which the administrative cost would exceed the connector time at stake. A maximum arrival state of charge $\sigma 0\max$ excludes vehicles that connect already close to the threshold, since these would collect a rebate for behavior they would have exhibited regardless, which is the standard free-rider problem in incentive design. The final condition restricts the transfer to periods in which site occupancy at the time of arrival reaches a minimum level U_{min}, so that connector time is recovered only when it has value; without it the operator pays for idleness, which is precisely the outcome shown to obtain at the installation studied here.

Threshold selection. The eighty per cent figure used in Section 4 is conventional and is not proposed as an operating threshold. Let $p(s)$ denote the mean delivered power observed at state of charge s, obtained from the minute-level telemetry of Section III-D, and let λ denote the operator's opportunity cost of connector time expressed as a delivery rate, that is, the rate below which occupying a connector ceases to be worthwhile given the demand the site faces. The threshold is then the lowest state of charge at which delivery has fallen to that rate,

$$s^* = \min\{\, s : \bar{p}(s) \le \lambda \,\} \qquad (10)$$

This ties the threshold to the taper characteristics of the fleet actually served and to the congestion actually experienced, rather than to convention. For the installation studied, $p(s)$ falls from approximately 93 kW near 30 per cent to approximately 19 kW above 95 per cent, so a demanding operator with λ = 40 kW would set s^* close to 80 per cent, while a tolerant one with λ = 25 kW would set it above 90. Section IV-D gives the corresponding share of connector-hours at each choice, and the two calculations together constitute the design procedure.

Expected relationship with disconnection behavior. The mechanism presumes that the probability of disconnecting at or below the threshold increases with the size of the transfer and saturates, which is the qualitative form reported by studies of driver response to charging and parking price signals [18], [19]. Writing $r(\pi)$ for the fraction of eligible drivers who disconnect at or below s^*, a bounded response of the form

$$r(\pi) = r_0 + (1 - r_0)(1 - e^{-\varepsilon\pi}) \qquad (11)$$

captures the two features any such relationship must have: a baseline $r0$, the fraction who already stop below the threshold without any incentive, which is measurable from the present record and equals 0.445 at s^* = 80 per cent; and saturation towards unity as the transfer grows, since the fraction cannot exceed one and since some drivers will not respond at any price. The parameter ε is the sensitivity of stopping behavior to the transfer and is the single unknown of the design. The recovered connector time follows as

Equation (11) is a hypothesis about behavior, not a result. No value of the sensitivity parameter is estimated here, and none can be, since the record contains no intervention. The exponential form is adopted because it is the simplest function satisfying the two boundary conditions the relationship must meet, namely that it equals the observed baseline at zero transfer and approaches unity as the transfer grows without bound. It is stated in this specific form so that a subsequent deployment study has a definite functional relationship to test and a single parameter to estimate; any other non-decreasing function meeting the same two conditions would serve, and the choice should be revisited once data on the response exists.

$$\Delta T(s^*, \pi) = r(\pi) \sum_{j \in \mathcal{E}} T_j^{>s^*} \qquad (12)$$

Equation (12) makes the earlier bound explicit and connects the mechanism to the measurement. At full compliance, r = 1, the recoverable time is the 176 to 215 connector-hours reported in Section 4-C, which is 17.1 to 20.9 per cent of all occupancy. At any realistic response it is a fraction of that. The measurement of Section 4 therefore fixes the ceiling of the mechanism independently of the behavioral parameter, which is the sense in which the diagnostic is useful before deployment rather than after it.

Deployment Conditions:

What the data do establish is the size of the target and the conditions under which pursuing it would be worthwhile. Two conditions matter.

The first is congestion. Recovered connector time has value only where demand exists to occupy it. This condition is not satisfied at the site studied: across the 448-day record the two connectors were occupied for 1,029 of 21,513 available connector-hours, so that U = 0.048 by equation (7), and both were simultaneously occupied for 1.0 per cent of wall-clock time. Recovery of 176 connector-hours would therefore yield 176 additional hours of idleness. Deployment is not justified at this site, and no saving is claimed on its behalf.

Figure 7 shows that this conclusion is not an artefact of averaging over a long record. Occupancy is concentrated in the working day, reaching 10.0 per cent in the busiest hour, and is distributed unevenly across the week. Even at the daily peak, occupancy remains far below the level at which one vehicle's departure would determine another's ability to charge.

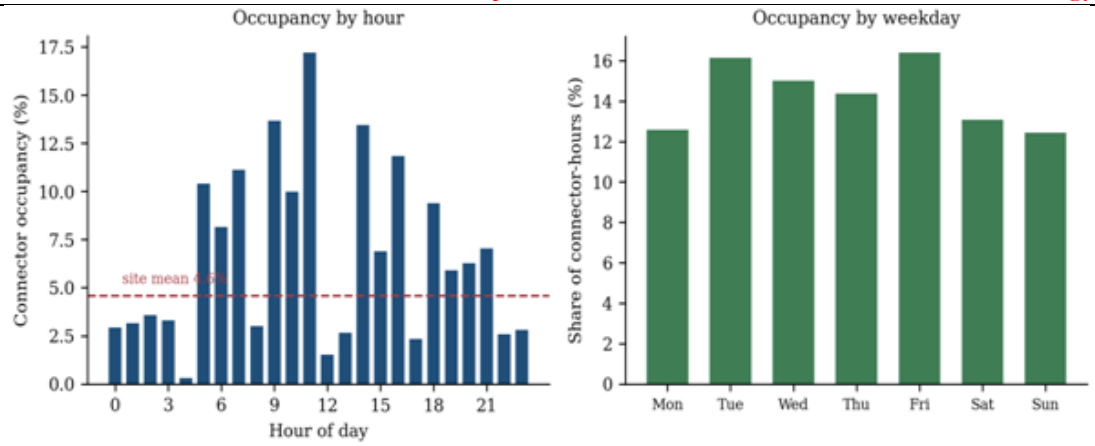


Figure 7. Connector occupancy by hour of day (left) and the distribution of connector-hours across weekdays (right). The dashed line marks the site mean of 4.6 per cent.

A site exhibiting the same session-level behavior at several times this occupancy would present a materially different case, and the recovered connector-hours would then translate into capacity rather than into idleness.

The second condition concerns the distribution of stopping behavior. An incentive can act only where drivers exercise discretion over the point of disconnection. At sites serving vehicles required to attain a high state of charge before departure, such as long-distance corridors or fleets operating on fixed rotations [11], the 55.5 per cent of sessions that continue past 80 per cent would not represent recoverable behavior, because the drivers concerned have no discretion to exercise. Section VI-A sharpens this condition: since none of the occupancy above the threshold is idle, the whole of it is discretionary charging or none of it is, and which obtains depends on the function the site serves.

The measurement is accordingly proposed as a diagnostic. It defines a quantity computable from records an operator already holds the share of connector-hours expended above a chosen threshold to be evaluated alongside the site occupancy rate before any such scheme is considered. Where occupancy is high and that share is large, the intervention point is substantial; where occupancy is low, as at the present site, it is not.

Discussion:

Decomposition of the Utilization Decline:

Sections 4-B and 4-E establish that connector utilization declines with the state of charge at disconnection and that delivered power declines over the same range. It does not follow that the charging curve accounts for the whole of the decline, and the distinction matters for the mechanism proposed here: an incentive acting on the point of disconnection addresses driver-controlled time, whereas a decline that is wholly physical would be irreducible by any behavioral instrument. The two can be separated arithmetically. Let T_j chg denote the connector time during which power actually flowed, obtained by counting minute-level observations with non-zero delivered power. Utilization then factors exactly as

$$\eta_j = \varphi_j \, \rho_j \qquad (13)$$

with

$$\varphi_j = \frac{T_j^{\text{chg}}}{T_j}, \qquad \rho_j = \frac{\bar{p}_j^{\text{chg}}}{P_j} = \frac{E_j}{T_j^{\text{chg}} P_j} \qquad (14)$$

The first factor, $\boldsymbol{\varphi j}$, is the fraction of the occupation during which any power flowed at all. It falls when a vehicle remains connected after charging has effectively ceased, which is behavior rather than physics: the driver has left the vehicle plugged in. The second factor, $\boldsymbol{\rho j}$, is the mean delivered power while charging, expressed as a fraction of the connector rating. It

falls as the cell enters the constant-voltage taper, which is physics and is not recoverable by any incentive. Because the factorization is exact and both factors are computable from the telemetry already used in Section 4-E, the relative contribution of the two mechanisms to the observed decline can be established directly rather than argued.

Table 4 reports the two factors by band. The result is unambiguous and was not the expected one. The factor φ is essentially constant, between 0.985 and 0.993 across every band, while ρ falls from 0.699 to 0.531 and accounts for the entire decline. Power flows for approximately 99 per cent of every connected period regardless of the state of charge at which the driver disconnects.

Table 4. Decomposition of connector utilization into the fraction of the occupation during which power flowed and the mean delivered rate.

SoC at disconnection (%)	n	η	φ (power flowing)	ϱ (rate)
< 60	317	0.688	0.985	0.699
60–70	173	0.683	0.992	0.689
70–80	345	0.663	0.993	0.668
80–90	496	0.610	0.992	0.615
90–95	183	0.569	0.993	0.573
> 95	362	0.526	0.991	0.531

Two conclusions follow, and the second matters more than the first. The decline in utilization with the state of charge at disconnection is attributable entirely to the charging curve; no part of it is idle connector time. Vehicles are not left connected after charging has effectively ceased at this site, and the explanation most readily reached for when a shared asset is underused is therefore excluded here by measurement rather than by argument.

It follows that the occupancy identified in Section 4-C is not waste in the ordinary sense. The 176 to 215 connector-hours expended above the eighty per cent threshold are spent delivering energy, at a rate that falls to under two thirds of that below the threshold, to drivers who have chosen to continue. This narrows the claim that can be made for any mechanism acting at the point of disconnection, and it is worth stating the narrowed claim precisely. The intervention cannot recover time during which nothing was happening, because there is none. What it can act on is the decision to continue charging into the region where the connector delivers least, which remains a decision the driver makes and which the measurement shows a majority of drivers make. The quantity at stake is unchanged; what changes is that the mechanism must be understood as altering a choice about charging rather than as reclaiming neglect.

Other Operational Factors:

Three further explanations for reduced utilization must be considered before the decline is attributed to the charging curve and to dwell behavior alone.

The first is session overhead. Authentication, handshake and cable-lock sequences occupy the connector before power flows and after it ceases. Section 6-A bounds this directly: power flows for between 98.5 and 99.3 per cent of the connected period in every band, so overhead accounts for at most 1.5 per cent of occupancy and cannot account for a mean utilization of 0.619. Its small residual effect on the reported gradient is in any case opposite in sign to the effect being measured, since a fixed per-session overhead depresses utilization most in short sessions, which are concentrated in the low-disconnection bands.

The second is thermal derating. A connector or a vehicle battery operating at elevated temperature will accept less power than its rating permits, and this is independent of the state of charge. Because it is driven by ambient conditions and by the duty cycle of the connector rather than by the point of disconnection, it would appear as variance within each band rather

than as a gradient across them, and it cannot generate a monotone relationship of the kind reported in Table 3.

The third is contention between the two connectors. Where a site shares a power module between connectors, simultaneous sessions can each receive less than the individual rating. This is excluded here on the evidence of Section 5-B: both connectors were simultaneously occupied for only 1.0 per cent of wall-clock time, which is far too infrequent to account for a mean utilization of 0.619 across the whole record.

None of the three can produce the monotone gradient reported, and the first works against it. Taken with the decomposition of Section 6-A, in which the idle factor is flat across all six bands, the decline is attributable to the charging curve alone.

Why the Site Occupancy Result Is Not a Negative Outcome

The installation studied fails both deployment conditions, and it would be possible to read that as a null result. It is better read as a demonstration of the diagnostic. The two quantities that determine whether the mechanism is worth deploying, the share of connector-hours above the threshold and the site occupancy rate, are computable from records every operator already keeps, and at this site they return a clear and actionable answer: do not deploy. An operator following the same procedure at a congested site would obtain the opposite answer with the same two calculations. The contribution is the procedure and the evidence that it discriminates, not the particular verdict returned here.

Implications:

For Charging-Station Operators:

The immediate implication for an operator is that connector availability can be assessed without capital expenditure. The two quantities that govern whether occupancy is recoverable, the share of connector-hours above a chosen threshold and the site occupancy rate, are computable from the session records that billing systems already generate, requiring only arrival and departure timestamps, delivered energy, connector rating and the states of charge at connection and disconnection. An operator considering an additional connector can therefore first establish how much of the existing connector time is being spent in the least productive region of the charging curve, and whether recovering it would relieve any actual constraint. At a congested site the calculation may show that a behavioral measure achieves what would otherwise require hardware; at an uncongested site, as here, it shows that neither is warranted, which is equally valuable in a capital-planning context.

A second implication concerns what operators should measure. Utilization reported as a site average conceals the composition that determines whether it is actionable. The factorization of equation (13) separates connector time during which no power flowed from time during which power flowed slowly, and the two call for entirely different responses. At the site studied the first factor is negligible, so no measure acting on dwell would recover anything; at a site where it is not, the same calculation would say so immediately. Reporting the two factors separately costs nothing beyond telemetry already collected and tells an operator which of the two problems they actually have.

For Infrastructure Planners:

For planners the implication concerns how site capability is estimated. Planning models conventionally convert a connector rating and an assumed utilization into a throughput figure. The present results indicate that the utilization term is not a site constant but depends on the distribution of disconnection states of charge among the vehicles served, which in turn depends on the function of the site. A corridor site serving vehicles that must reach a high state of charge before departure will exhibit systematically lower connector utilization than a destination site serving opportunistic top-ups, at identical hardware and identical demand. Planning that treats utilization as a hardware property will therefore

overstate the capability of corridor sites relative to destination sites, and the magnitude of the error is indicated by the spread reported here, from 0.688 to 0.526 across disconnection bands.

A related implication is that connector count and connector rating are not interchangeable. At this installation the connector is the binding constraint in every session, with a median of 86 kW of vehicle demand unserved, so raising the rating would shorten sessions and raise throughput per connector. Where sessions instead extend into the taper, additional rating delivers progressively less, because the vehicle rather than the connector then sets the rate.

For Electric-Vehicle Users:

For drivers the implication is that the cost of charging to a high state of charge at a fast-charging site borne in the form of additional charging time, and that the time is disproportionate to the energy obtained. In this record, sessions continuing past 80 per cent spent between 176 and 215 connector-hours to deliver a median of 7.1 kWh each, at under two thirds of the throughput per minute of the charge below that threshold. A driver who disconnects at the threshold and completes charging at a destination or overnight incurs little practical penalty in range while spending materially less time at the connector. Where a site is congested, that choice also releases capacity to other users, which is the externality the proposed mechanism would internalize.

Recommendations:

The following recommendations follow from the results and are stated so that they can be acted upon or contradicted.

Threshold Selection:

Operators should not adopt the eighty per cent convention as an operating threshold. It is a reporting convention drawn from manufacturer guidance and it has no operational meaning at a specific site. The threshold should instead be set by equation (10), as the lowest state of charge at which the mean delivered power observed in the operator's own telemetry has fallen to the operator's opportunity cost of connector time. Section 4-D shows why these matters: the share of connector-hours above the threshold varies from 32.1 per cent at 70 per cent to 5.7 per cent at 90 per cent, so the choice of threshold changes the size of the target by a factor exceeding five. Any figure quoted without its threshold is uninterruptable.

Incentive Deployment:

Deployment should be conditional rather than general. The occupancy charge of equation (8) should be applied only to sessions in the eligible set of equation (9), and in particular only during periods in which site occupancy reaches the minimum level. An incentive applied at all hours would pay for connector time that has no alternative use, converting a transfer into a pure cost. Where an operator cannot vary price, the priority-entitlement form is recommended in preference, since it carries no revenue implication and is not subject to the same regulatory constraints on tariff structure. In either form the transfer should be indexed to occupancy above the threshold rather than to energy delivered, so that it prices the resource actually consumed.

Site Occupancy Requirements:

A minimum occupancy condition should be verified before any such scheme is contemplated. On the evidence presented here a site occupancy of 4.6 per cent is decisively insufficient: recovering 176 connector-hours at this installation would yield 176 additional hours of idleness. The condition should be assessed at the resolution at which contention actually occurs, not as a record-long average, since a site can be congested at its daily peak while appearing idle overall. At this installation the peak-hour occupancy of 10.0 per cent and the 1.0 per cent of wall-clock time with both connectors busy both fail the condition, so the conclusion holds at every resolution examined. We suggest that operators report peak-hour occupancy and simultaneous occupancy alongside the mean.

Future Validation through Intervention:

The single unknown in the design is the response parameter of equation (11), and it cannot be estimated from observational data. We recommend a staged intervention study at a site meeting both deployment conditions. A pre-intervention period establishes the baseline distribution of disconnection states of charge and the value of η_0. The incentive is then introduced at a single threshold with a fixed transfer, ideally with concurrent control connectors at a comparable site so that seasonal and fleet-composition effects are differenced out. The quantity to be estimated is the shift in the distribution of the disconnection state of charge, not the change in mean utilization, since the latter confounds the behavioral response with changes in the arrival mix. Varying the transfer across periods would in addition identify ε rather than merely establishing that a response exists. Until such a study is conducted, the mechanism proposed here should be regarded as a specified hypothesis and not as a validated intervention.

Limitations:

Four limitations bear on the interpretation of these results. The analysis covers a single installation with two connectors over fifteen months. The composition of occupancy reported here depends on the fleet served and on the power rating of the connectors, and neither is representative by construction. A site serving vehicles with different taper characteristics, or connectors rated close to the power requested by the vehicles using them**,** would yield a different decomposition; the second case would in addition violate the condition that the connector is everywhere the binding constraint.

The time attributable to charging above a threshold, defined by equation (5), is estimated from the session mean delivered rate rather than measured directly. Because delivery slows in the region concerned, this estimator understates the time attributable to it. Section IV-C therefore reports both the lower bound obtained from the session mean and the upper bound obtained from the measured taper rate, and the share should be read as the interval between them rather than as a point estimate.

The state of charge at disconnection is reported by the vehicle and is not independently verified. Errors in that quantity propagate into equation (4) and hence into equations (5) and (6), and they do so without attenuation, since Section III-C establishes that the capacity term is itself a function of the reported states of charge. Two sessions were excluded on this basis.

No intervention is present in the record. The incentive outlined above is therefore proposed rather than evaluated, and no estimate of driver response is offered. Establishing such an estimate requires a site at which an incentive is deployed and behavior is observed before and after.

A fifth limitation follows from Section III-B. The power term in equation (1) is the maximum delivered during the session rather than a nameplate rating, since the record supplies the former and not the latter. Utilization as reported is therefore relative to what the connector achieved rather than to what it is rated to achieve. A nameplate denominator would be at least as large, so the utilization figures here are conservative, but they are not directly comparable with studies computing the ratio against a catalogue rating.

Conclusion:

Using 1,876 sessions from a two-connector direct-current fast-charging installation, this paper decomposed connector occupancy rather than forecasting it. Delivery was limited at the connector in every session recorded, with a median of 86 kW of vehicle demand left unserved, which removes vehicle-side limitation as an explanation for a mean utilization of 0.619. Utilization instead falls monotonically with the state of charge at disconnection, from 0.688 below 60 per cent to 0.526 above 95, a decline confirmed as ordered by a Jonckheere–Terpstra test at $p < 10^{-96}$, and the 55.5 per cent of sessions continuing past 80 per cent consume between 17.1 and 20.9 per cent of all connector-hours at under two thirds of the

throughput per minute of the charge below that threshold. Minute-level telemetry establishes that this occupancy is not idle: power flows for approximately 99 per cent of every connected period in every band, so the decline is attributable to the charging curve alone and the target of any intervention is the decision to continue charging rather than the neglect of a connector. An incentive indexed to the state of charge at disconnection rather than to time of day was outlined at concept level, together with the two site conditions, congestion and discretionary stopping behavior, under which its evaluation would be warranted. The site studied satisfies neither, exhibiting an occupancy of 4.8 per cent. The measurement is therefore offered as a diagnostic computable from existing operational records prior to considering such a scheme. Estimation of driver response requires a deployment and is reserved for future work.

References:

[1] Z. Jin, H. Li, D. Chen, L. Yu, and H. Tu, "Accounting for BEV Users' Risk Attitudes and Charging Inertia in En Route Charging Choice Behavior," *J. Adv. Transp.*, vol. 2024, no. 1, p. 9926334, Jan. 2024, doi: 10.1155/2024/9926334.

[2] S. Gohlke and Z. Nochta, "Short-Term Utilization Forecasting of Electric Vehicle Charging Infrastructures," *World Electr. Veh. J. 2025, Vol. 16, Page 655*, vol. 16, no. 12, p. 655, Nov. 2025, doi: 10.3390/WEVJ16120655.

[3] M. Rashid, T. Elfouly, and N. Chen, "A Comprehensive Survey of Electric Vehicle Charging Demand Forecasting Techniques," *IEEE Open J. Veh. Technol.*, vol. 5, pp. 1348–1373, 2024, doi: 10.1109/OJVT.2024.3457499.

[4] R. Wolbertus and R. Van den Hoed, "Electric Vehicle Fast Charging Needs in Cities and along Corridors," *World Electr. Veh. J. 2019, Vol. 10, Page 45*, vol. 10, no. 2, p. 45, Jun. 2019, doi: 10.3390/WEVJ10020045.

[5] C. Hecht, J. Figgener, and D. U. Sauer, "Analysis of electric vehicle charging station usage and profitability in Germany based on empirical data," *iScience*, vol. 25, no. 12, p. 105634, Dec. 2022, doi: 10.1016/J.ISCI.2022.105634.

[6] A. Rautiainen *et al.*, "Anatomy of electric vehicle fast charging: Peak shaving through a battery energy storage—A case study from Oslo," *IET Electr. Syst. Transp.*, vol. 11, no. 1, pp. 69–80, Mar. 2021, doi: 10.1049/ELS2.12005.

[7] M. Neaimeh, S. D. Salisbury, G. A. Hill, P. T. Blythe, D. R. Scoffield, and J. E. Francfort, "Analysing the usage and evidencing the importance of fast chargers for the adoption of battery electric vehicles," *Energy Policy*, vol. 108, pp. 474–486, Sep. 2017, doi: 10.1016/J.ENPOL.2017.06.033.

[8] J. R. Helmus, M. H. Lees, and R. van den Hoed, "A data driven typology of electric vehicle user types and charging sessions," *Transp. Res. Part C Emerg. Technol.*, vol. 115, p. 102637, Jun. 2020, doi: 10.1016/J.TRC.2020.102637.

[9] S. Hardman *et al.*, "A review of consumer preferences of and interactions with electric vehicle charging infrastructure," *Transp. Res. Part D Transp. Environ.*, vol. 62, pp. 508–523, Jul. 2018, doi: 10.1016/J.TRD.2018.04.002.

[10] T. Gnann, S. Funke, N. Jakobsson, P. Plötz, F. Sprei, and A. Bennehag, "Fast charging infrastructure for electric vehicles: Today's situation and future needs," *Transp. Res. Part D Transp. Environ.*, vol. 62, pp. 314–329, Jul. 2018, doi: 10.1016/J.TRD.2018.03.004.

[11] R. Wolbertus, M. Kroesen, R. van den Hoed, and C. G. Chorus, "Policy effects on charging behaviour of electric vehicle owners and on purchase intentions of prospective owners: Natural and stated choice experiments," *Transp. Res. Part D Transp. Environ.*, vol. 62, pp. 283–297, Jul. 2018, doi: 10.1016/J.TRD.2018.03.012.

[12] C. Hecht, J. Figgener, and D. U. Sauer, "Predicting Electric Vehicle Charging Station Availability Using Ensemble Machine Learning," *Energies 2021, Vol. 14, Page 7834*,

vol. 14, no. 23, p. 7834, Nov. 2021, doi: 10.3390/EN14237834.

[13] D. Matkovic, I. Sudic, and T. Capuder, "Day-ahead and intra-day forecasting of electric vehicle charging station energy consumption," *2023 8th Int. Conf. Smart Sustain. Technol. Split. 2023*, 2023, doi: 10.23919/SPLITECH58164.2023.10193158.

[14] E. Apostolaki-Iosifidou, P. Codani, and W. Kempton, "Measurement of power loss during electric vehicle charging and discharging," *Energy*, vol. 127, pp. 730–742, May 2017, doi: 10.1016/J.ENERGY.2017.03.015.

[15] I. Ullah, K. Liu, T. Yamamoto, M. Zahid, and A. Jamal, "Prediction of electric vehicle charging duration time using ensemble machine learning algorithm and Shapley additive explanations," *Int. J. Energy Res.*, vol. 46, no. 11, pp. 15211–15230, Sep. 2022, doi: 10.1002/ER.8219.

[16] F. Alanazi, "Electric Vehicles: Benefits, Challenges, and Potential Solutions for Widespread Adaptation," *Appl. Sci. 2023, Vol. 13, Page 6016*, vol. 13, no. 10, p. 6016, May 2023, doi: 10.3390/APP13106016.

[17] Y. A. Khan *et al.*, "Enhancing Smart Home Efficiency with Heuristic-Based Energy Optimization," *Comput. 2025, Vol. 14, Page 149*, vol. 14, no. 4, p. 149, Apr. 2025, doi: 10.3390/COMPUTERS14040149.

[18] C. Latinopoulos, A. Sivakumar, and J. W. Polak, "Response of electric vehicle drivers to dynamic pricing of parking and charging services: Risky choice in early reservations," *Transp. Res. Part C Emerg. Technol.*, vol. 80, pp. 175–189, Jul. 2017, doi: 10.1016/J.TRC.2017.04.008.

[19] S. Limmer, "Dynamic Pricing for Electric Vehicle Charging—A Literature Review," *Energies 2019, Vol. 12, Page 3574*, vol. 12, no. 18, p. 3574, Sep. 2019, doi: 10.3390/EN12183574.

[20] Z. J. Lee, T. Li, and S. H. Low, "ACN-Data: Analysis and applications of an open EV charging dataset," *e-Energy 2019 - Proc. 10th ACM Int. Conf. Futur. Energy Syst.*, pp. 139–149, Jun. 2019, doi: 10.1145/3307772.3328313;.

[21] O. I. Asensio, C. Z. Apablaza, M. C. Lawson, and S. E. Walsh, "A field experiment on workplace norms and electric vehicle charging etiquette," *J. Ind. Ecol.*, vol. 26, no. 1, pp. 183–196, Feb. 2022, doi: 10.1111/JIEC.13116;.

[22] Z. Lu, Q. Zhang, Y. Yuan, and W. Tong, "Optimal Driving Range for Battery Electric Vehicles Based on Modeling Users' Driving and Charging Behavior," *J. Adv. Transp.*, vol. 2020, no. 1, p. 8813137, Jan. 2020, doi: 10.1155/2020/8813137.

[23] O. Frendo, N. Gaertner, and H. Stuckenschmidt, "Open Source Algorithm for Smart Charging of Electric Vehicle Fleets," *IEEE Trans. Ind. Informatics*, vol. 17, no. 9, pp. 6014–6022, Sep. 2021, doi: 10.1109/TII.2020.3038144.

[24] M. F. Voss, S. P. Haveman, and G. M. Bonnema, "In-Company Smart Charging: Development of a Simulation Model to Facilitate a Smart EV Charging System," *Energies 2021, Vol. 14, Page 6723*, vol. 14, no. 20, p. 6723, Oct. 2021, doi: 10.3390/EN14206723.

[25] K. V. Sastry, S. Holla, S. Tater, E. Gustafson, D. G. Taylor, and M. J. Leamy, "Design and Demonstration of a Smart Charging System for Plug-in Electric Vehicles," *2023 IEEE Transp. Electrif. Conf. Expo, ITEC 2023*, 2023, doi: 10.1109/ITEC55900.2023.10186905.

[26] N. I. Nimalsiri, C. P. Mediwaththe, E. L. Ratnam, M. Shaw, D. B. Smith, and S. K. Halgamuge, "A Survey of Algorithms for Distributed Charging Control of Electric Vehicles in Smart Grid," *IEEE Trans. Intell. Transp. Syst.*, vol. 21, no. 11, pp. 4497–4515, Nov. 2020, doi: 10.1109/TITS.2019.2943620.

[27] J. Y. Yong, V. K. Ramachandaramurthy, K. M. Tan, and N. Mithulananthan, "A review on the state-of-the-art technologies of electric vehicle, its impacts and

prospects," *Renew. Sustain. Energy Rev.*, vol. 49, pp. 365–385, Sep. 2015, doi: 10.1016/J.RSER.2015.04.130.

[28] A. Tomaszewska *et al.*, "Lithium-ion battery fast charging: A review," *eTransportation*, vol. 1, p. 100011, Aug. 2019, doi: 10.1016/J.ETRAN.2019.100011.

[29] P. M. Attia *et al.*, "Closed-loop optimization of fast-charging protocols for batteries with machine learning," *Nat. 2020 5787795*, vol. 578, no. 7795, pp. 397–402, Feb. 2020, doi: 10.1038/s41586-020-1994-5.

Copyright © by authors and 50Sea. This work is licensed under Creative Commons Attribution 4.0 International License.